

## Microdroplet Ultrafast Reactions Speed Antibody Characterization

Pengyi Zhao, Harsha P. Gunawardena,\* Xiaoqin Zhong, Richard N. Zare,\* and Hao Chen\*

Cite This: *Anal. Chem.* 2021, 93, 3997–4005

Read Online

ACCESS |



Metrics &amp; More

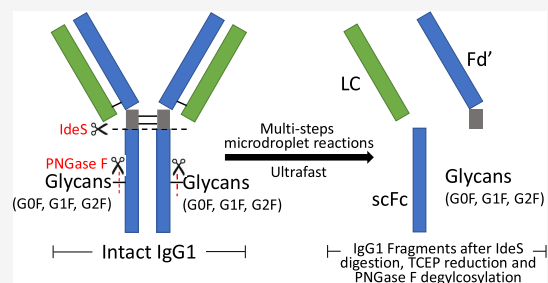


Article Recommendations



Supporting Information

**ABSTRACT:** Recently, microdroplet reactions have aroused much interest because the microdroplet provides a unique medium where organic reactions could be accelerated by a factor of  $10^3$  or more. However, microdroplet reactions of proteins have been rarely studied. We report the occurrence of multiple-step reactions of a large protein, specifically, the digestion, reduction, and deglycosylation of an intact antibody, which can take place in microseconds with high reaction yields in aqueous microdroplets at room temperature. As a result, fast structural characterization of a monoclonal antibody, essential for assessing its quality as a therapeutic drug, can be enabled. We found that the IgG1 antibody can be digested completely by the IdeS protease in aqueous microdroplets in 250 microseconds, a 7.5 million-fold improvement in speed in comparison to traditional digestion in bulk solution ( $>30$  min). Strikingly, inclusion of the reductant tris(2-carboxyethyl)phosphine in the spray solution caused simultaneous antibody digestion and disulfide bond reduction. Digested and reduced antibody fragments were either collected or analyzed online by mass spectrometry. Further addition of PNGase F glycosylase into the spray solution led to antibody deglycosylation, thereby producing reduced and deglycosylated fragments of analytical importance. In addition, glycosylated fragments of IgG1 derived from glucose modification were identified rapidly with this ultrafast digestion/reduction technique. We suggest that microdroplets can serve as powerful microreactors for both exploring large-molecule reactions and speeding their structural analyses.



## INTRODUCTION

Microdroplets have been recently found to be a unique reaction media in which reaction acceleration can occur.<sup>1</sup> It has aroused much attention in the field of chemistry and has been extensively investigated.<sup>2–22</sup> Various reactions of organic molecules are markedly promoted in sprayed micron-sized droplets (microdroplets) compared with the same reactions in bulk-phase solution.<sup>23</sup> Numerous explanations have been offered for why reaction rate acceleration occurs in aqueous microdroplets. These explanations include evaporation, increased autoionization, partial desolvation, presence of an intrinsic strong electric field at the interface, enhanced concentration of solutes on the surface of the microdroplet, and restricted orientations.<sup>24–33</sup> The factors that are dominant in any given situation still need to be identified. However, most previous work focused on one-step reactions of small molecules. Biochemical reactions involving proteins have been rarely investigated, except a recent report of trypsin digestion of proteins in microdroplets.<sup>34</sup>

Therapeutic monoclonal antibodies (mAbs) are one of the fastest growing classes of drugs. More than one hundred mAbs for treatment of many pathologies such as cancer and autoimmune diseases have been approved or are in regulatory review in the US and EU.<sup>35,36</sup> This ever-growing abundance has created a need for rapid technologies to characterize mAbs to secure drug product safety, quality, and efficacy.<sup>37–39</sup> Traditional mass spectrometry (MS) mAb characterization

methods include intact and subunit mass analyses and peptide mapping.<sup>40–44</sup> To characterize mAbs in a bottom-up or middle-down proteomics approach, mAbs must be subjected to enzymatic digestion into peptides or polypeptides before peptide mapping analysis by MS. However, digestion is usually a time-consuming step that can take from 30 min to overnight incubation.<sup>45,46</sup> In addition, commonly used digestion methods often include additional steps of protein denaturation, reduction, and alkylation to unfold the mAb structure and facilitate digestion; these additional steps may also lengthen the process time and reduce the analysis speed and throughput.<sup>47</sup> To accelerate digestion of mAb (or other proteins), a variety of methods have been investigated, including increasing the digestion temperature, adding organic solvents, applying microwave energy, using high-intensity focused ultrasound, or employing a microchip reactor.<sup>48–56</sup> Nevertheless, an alternative method that is very fast for mAb digestion would be highly valuable.

In this study, we present unprecedented and fast microdroplet reactions involving a large protein substrate (i.e., an

Received: November 26, 2020

Accepted: February 5, 2021

Published: February 16, 2021



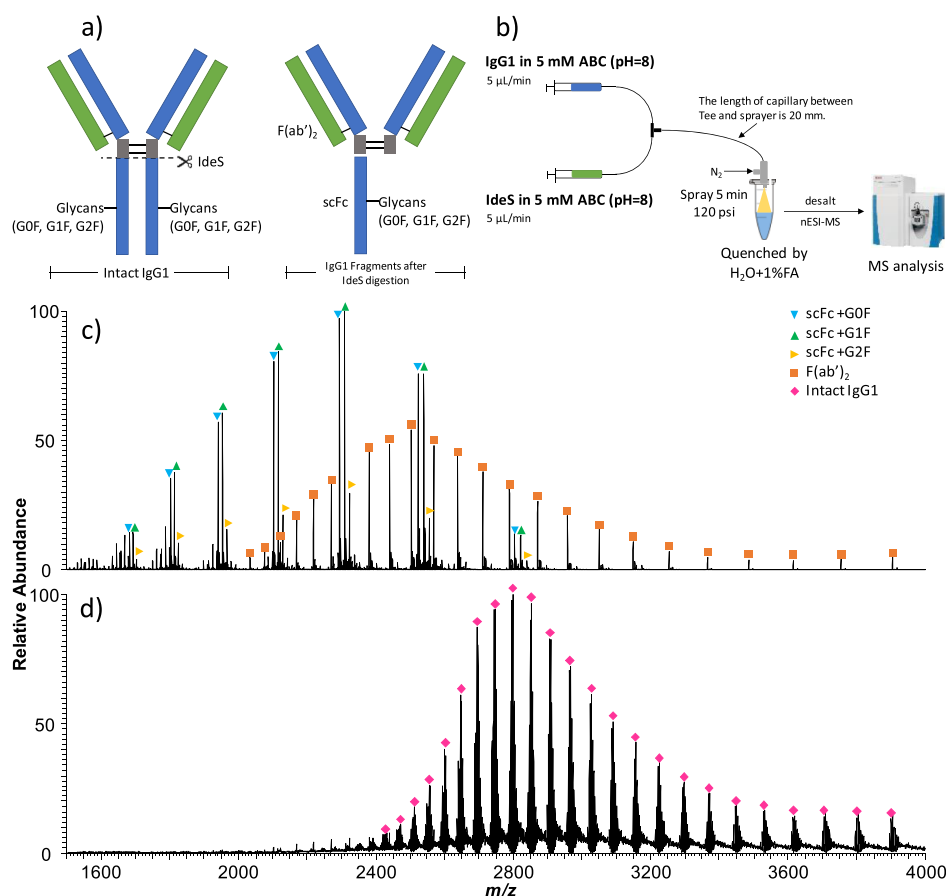


**Figure 1.** Microdroplet digestion of IgG1 (the NIST IgG1 monoclonal antibody reference material 8671) by the IdeS enzyme: (a) Schematic drawing of intact IgG1 and IdeS-cleaved IgG1 fragments; the LC, heavy chain, and hinge region are highlighted in green, blue, and gray, respectively. Black solid lines indicate disulfide bonds connecting heavy chain and LC. The IdeS cleavage site is indicated with a scissors and a dash line. (b) Workflow of microdroplet digestion of IgG1 by IdeS; nESI-MS spectra of (c) antibody fragments obtained from microdroplet digestion of IgG1 by IdeS at room temperature and (d) in-solution digested IgG1 by IdeS for 5 min at 37 °C.

antibody), which would have high impact in proteomics for rapid characterization of antibodies. In this work, ultrafast digestion of the NIST IgG1 antibody in 250 microseconds in microdroplets was achieved. The IgG1 was selectively cleaved by IdeS protease into antigen-binding fragment F(ab')<sub>2</sub> and single-chain, crystallizable fragment scFc (Figure 1a). When we included the reductant tris(2-carboxyethyl)phosphine (TCEP) in the spray solution, simultaneous disulfide bond reduction occurred, leading to digested and reduced IgG1 fragments that included light chain (LC), N-terminal half of heavy chain Fd', and scFc subunits (Figure 2a). These fragments could be either collected for further analysis or detected online by MS. In addition, we achieved ultrafast deglycosylation of IgG1 by including PNGase F glycosylase in the microdroplets (Figure 4a), which constituted an alternative method to rapidly remove glycans from antibodies. In addition, following incubation with glucose, we successfully digested and characterized glycosylated IgG1 fragments in microdroplets, which suggested a fast way to detect antibody modifications in general.

## EXPERIMENTAL SECTION

**Chemicals.** NIST monoclonal antibody reference material 8671 (NIST mAb, humanized IgG1k monoclonal antibody) was obtained from the National Institute of Standards and Technology (Gaithersburg, MD). The IdeS enzyme was purchased from Genovis Inc (Cambridge, MA). TCEP

hydrochloride (bioultra grade), ammonium bicarbonate (bioultra grade), sodium phosphate dibasic (bioultra grade), and sodium phosphate monobasic (bioultra grade) were purchased from Sigma-Aldrich (St. Louis, MO). D-(+)-Glucose (98% purity) was obtained from TCI America (Montgomeryville, PA). Acetonitrile (ACN, HPLC grade), formic acid (FA, LCMS grade), and trifluoroacetic acid (TFA, LCMS grade) were purchased from Fisher Scientific (Fair Lawn, NJ). A Millipore Direct-Q5 purification system (Burlington, MA) was used to obtain purified water for sample preparation.

**Microdroplet Generation.** Microdroplets were generated by spraying an aqueous sample solution (NIST IgG1 mixed with IdeS, TCEP, PNGase F, or all reagents together) through a home-made sprayer with the assistance of nitrogen gas as a sheath gas at 120 psi. The home-made sprayer was built exactly as previously described for an electrosonic spray source.<sup>57</sup> Briefly, the aqueous sample solution was delivered through a fused-silica capillary (100 μm i.d. and 200 μm o.d., Polymicro Technologies, Phoenix, AZ). Another coaxial fused-silica outer capillary (250 μm i.d. and 300 μm o.d.) was used, and the small size difference between two capillaries was capable of providing nebulizing gas at high velocity.<sup>14</sup> Based on the previous reports,<sup>14,34</sup> such a sprayer with the use of 120 psi nitrogen nebulization gas pressure produces small microdroplets of 13 ± 6 μm in diameter which is critical for

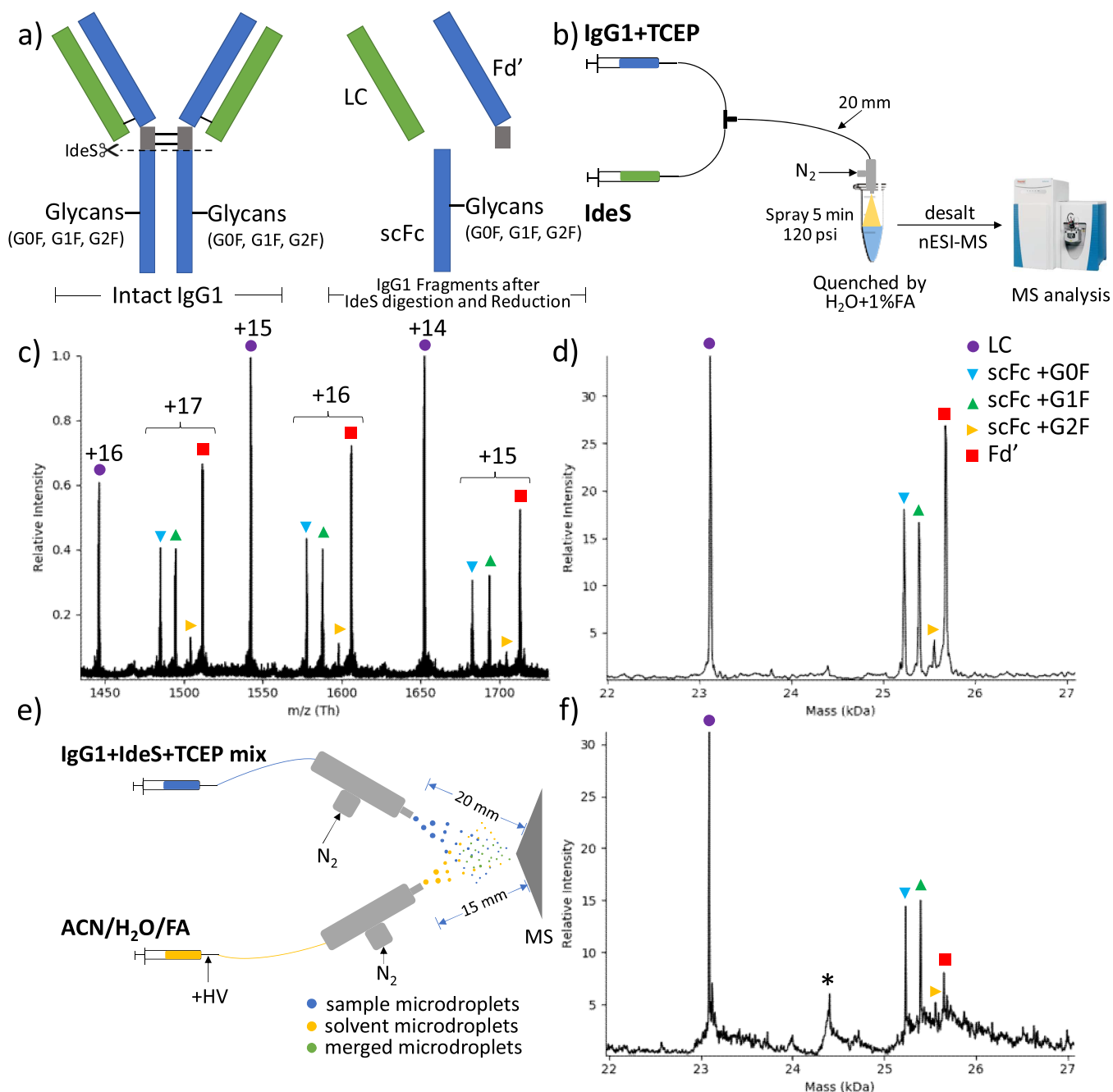


**Figure 2.** Simultaneous microdroplet digestion and reduction of IgG1. (a) Schematic representation of intact IgG1 and fragment structures of IgG1 after IdeS digestion and TCEP reduction. (b) Schematic drawing of the microdroplet digestion and reduction workflow. (c) Expanded MS spectrum with LC, Fd', and glycosylated scFc fragments detected and annotated. (d) Corresponding deconvoluted MS spectrum of (c). (e) Schematic drawing of simultaneous microdroplet digestion and reduction coupled with online EESI-MS detection. (f) Deconvoluted MS spectrum of digested and reduced IgG1 from online EESI-MS detection. Note that asterisk (\*) in (f) denotes a harmonic peak of Fab [equivalent to half of  $F(ab')_2$ ].

achieving the reaction acceleration effect in microdroplets. The sprayer does not need an applied voltage.

**Microdroplet Digestion with nESI-MS Analysis.** For the experiment shown in Figure 1b, 50  $\mu$ L of 1 mg/mL IgG1 in 5 mM  $\text{NH}_4\text{HCO}_3$  buffer (pH 8) was loaded in one syringe. Then, 50  $\mu$ L of 2 units/ $\mu$ L IdeS enzyme in 5 mM  $\text{NH}_4\text{HCO}_3$  buffer (pH 8) was loaded in the other syringe. The flow rate of both the syringes was 5  $\mu$ L/min, and the reactants were mixed by a Tee. The length of the capillary between the mixing Tee and the sprayer was 2 cm. The microdroplets were generated

through the sprayer and collected in a vial containing a quenching solvent of 50  $\mu$ L of  $\text{H}_2\text{O}$  and 1% FA. The distance between the sprayer tip and the surface of the quenching solution was 20 mm. After 5 min collection, desalting and reagent removal was performed with a C4 Ziptip (MilliporeSigma, Burlington, MA). The desalted sample was analyzed by nano-electrospray ionization (nESI) in front of a Q Exactive Orbitrap mass spectrometer (Thermo Scientific, San Jose, CA). The injection flow rate was 2  $\mu$ L/min, and +3 kV was applied for ionization. The temperature of the MS inlet

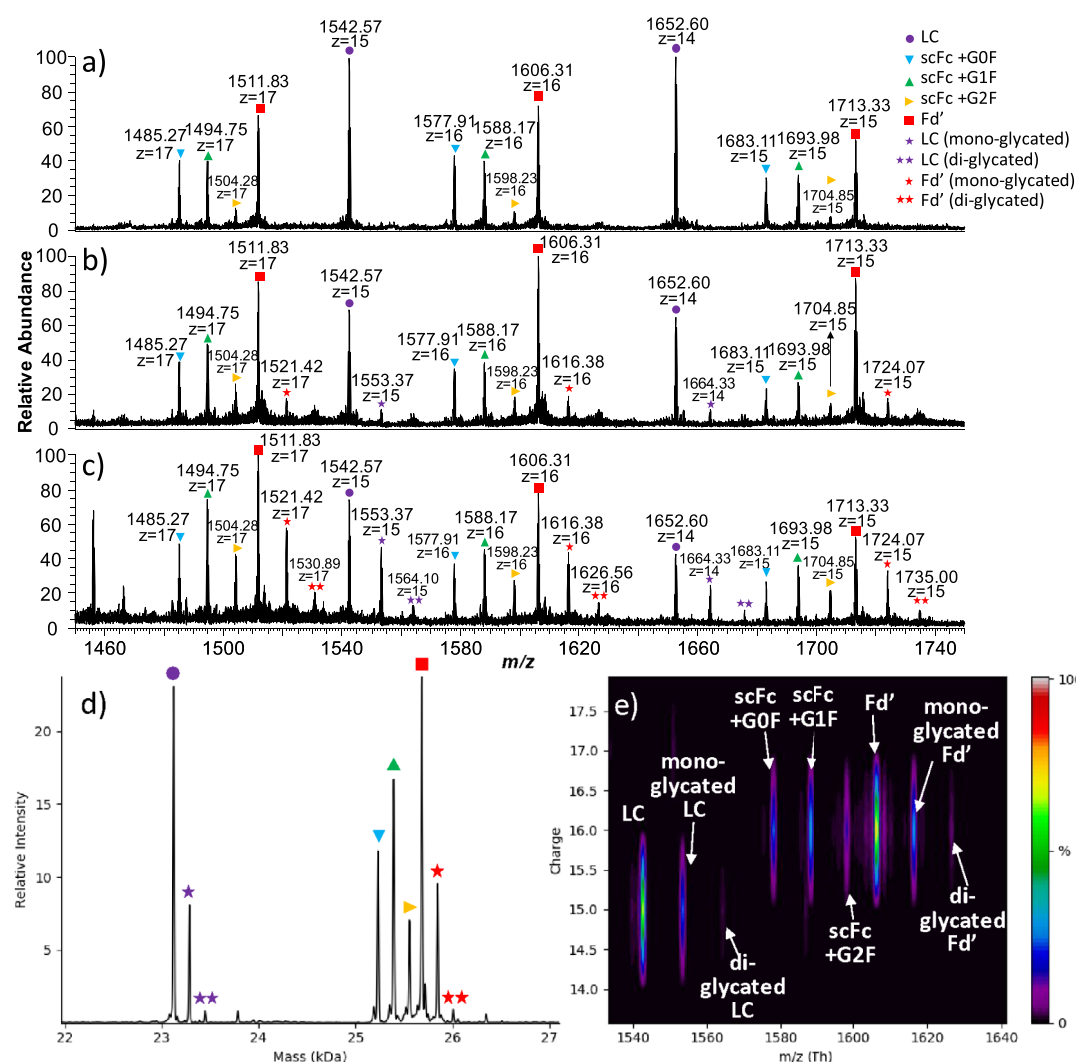


**Figure 3.** Microdroplet digestion and reduction for analysis of glycosylated IgG1. In this “one-pot reaction” approach, glycosylated IgG1, IdeS, and TCEP were mixed and reacted together. The subunits of LC (and glycosylated-LC), Fd' (and glycosylated-Fd'), and scFc fragments were produced simultaneously. (a) Expanded view of the MS spectrum of nonglycosylated IgG1 (at day 0) after microdroplet digestion and reduction; (b) MS spectrum of glycosylated IgG1 (incubated with glucose for 2 days) after microdroplet digestion and reduction; (c) MS spectrum of glycosylated IgG1 (incubated with glucose for 5 days) after microdroplet digestion and reduction; (d) deconvoluted MS spectrum of glycosylated IgG1 after 5 days of incubation and microdroplet reactions; and (e) 2D spectrum of glycosylated IgG1 after 5 days of incubation and microdroplet reactions, with  $m/z$  along the  $x$ -axis and charge number along the  $y$ -axis.

was 250 °C. The mass spectrometer resolution was set to 17,500 for the MS analysis. All sample mixing and injecting steps were performed rapidly without delay time between each step to avoid reaction occurring in the bulk solution under ambient temperature. For the experiment in Figure 2b, 50  $\mu\text{L}$  of 1 mg/mL IgG1 in 5 mM  $\text{NH}_4\text{HCO}_3$  buffer containing 5 mM TCEP (pH 8) was loaded in one syringe. Then, 50  $\mu\text{L}$  of 2 units/ $\mu\text{L}$  IdeS enzyme in 5 mM  $\text{NH}_4\text{HCO}_3$  buffer (pH 8) was loaded in the other syringe. The remaining steps were the same as the steps in the aforesaid Figure 1b experiment.

**Microdroplet Digestion with Online EESI-MS Analysis.** In the online workflow, the extractive electrospray ionization mass spectrometry (EESI-MS) method reported by Chen and co-workers<sup>58</sup> was adopted with minor modifications. The schematic drawing is shown in Figure 2e. Briefly, one sprayer was used to generate microdroplets from a one-pot mixture of NIST IgG1, IdeS, and TCEP solution without applying any voltage. The mixed sample solution consisted of 5  $\mu\text{L}$  of 10 mg/mL NIST IgG1, 2  $\mu\text{L}$  of 50 units/ $\mu\text{L}$  IdeS

enzyme, and 93  $\mu\text{L}$  of 5 mM  $\text{NH}_4\text{HCO}_3$  buffer containing 5 mM TCEP. The other sprayer emitted ACN/ $\text{H}_2\text{O}$ /FA solvent (50:50:0.5%), and +3 kV voltage was applied to the solvent through a metal alligator clip attached to the stainless steel tip of the syringe used for solvent infusion. The flow rate of both the sprayers was 10  $\mu\text{L}/\text{min}$ . The pressure of nitrogen gas for both the sprayers was 120 psi. The distance between the tip of the solvent sprayer and the MS inlet was 15 mm, and the distance between the tip of the mixed sample sprayer and the MS inlet was 20 mm. The EESI source was aligned carefully to the MS inlet to achieve the highest sensitivity. The temperature of the MS inlet was 250 °C.

**Glycosylated IgG1 Characterization.** Twenty microliters of 10 mg/mL NIST IgG1 was added to 180  $\mu\text{L}$  of 200 mM  $\text{NH}_4\text{HCO}_3$  buffer containing 200 mM glucose (pH 8). The final concentration of IgG1 was 1 mg/mL. Then, the sample solution was incubated at 37 °C for 0, 2, and 5 days. After incubation, 10  $\mu\text{L}$  of 1 mg/mL glycosylated IgG1 was drawn out and mixed with 2  $\mu\text{L}$  of 50 units/ $\mu\text{L}$  IdeS in 88  $\mu\text{L}$  of 5 mM

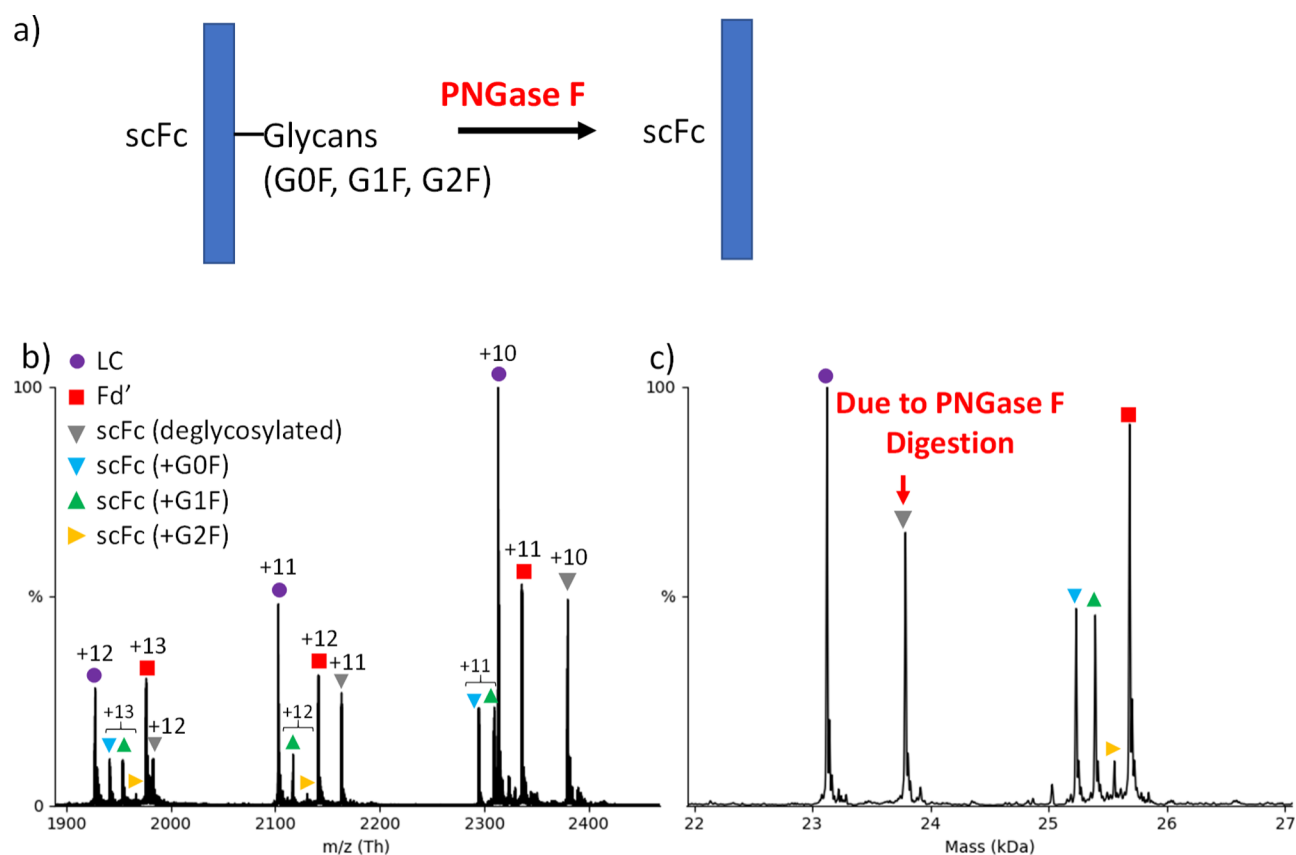


**Figure 4.** “One-pot” microdroplet reactions with IgG1, PNGase F, IdeS, and TCEP. (a) Schematic illustrating the PNGase F deglycosylation; (b) expanded MS spectrum with LC, Fd', and scFc (both deglycosylated and glycosylated) fragments detected and annotated; (c) deconvoluted MS spectrum of (b).

$\text{NH}_4\text{HCO}_3$  buffer containing 5 mM TCEP (pH 8). The final concentration of glycosylated IgG1 was 0.1 mg/mL in the resulting mixture, which was sprayed to trigger microdroplet reactions at a flow rate of 10  $\mu\text{L}/\text{min}$  for 5 min. Then, 50  $\mu\text{L}$  of  $\text{H}_2\text{O}$  containing 0.1% TFA was added to reconstitute the collected microdroplets and terminate the enzymatic reaction. Desalting and reagent removal was performed with a C4 Ziptip. The desalted sample was analyzed by nESI using the Q Exactive Orbitrap mass spectrometer. The injection flow rate was 2  $\mu\text{L}/\text{min}$ , and +3 kV was applied for ionization. The temperature of the MS inlet was 250  $^\circ\text{C}$ .

**Deglycosylation of IgG1 by PNGase F.** Five microliters of 10 mg/mL NIST IgG1 was mixed with 45 microliters of 5 mM  $\text{NH}_4\text{HCO}_3$  buffer (pH 8) and loaded in one syringe. The final concentration of IgG1 was 1 mg/mL. Then, 100  $\mu\text{L}$  of 1 unit/ $\mu\text{L}$  mM PNGase F in 5 mM  $\text{NH}_4\text{HCO}_3$  buffer (pH 8) was loaded in the other syringe. The remaining steps were the same as the steps in the aforesaid Figure 1b experiment.

## RESULTS AND DISCUSSION

We first investigated the direct microdroplet digestion of IgG1 by the IdeS enzyme. The IdeS enzyme, cloned from *Streptococcus pyogenes* and expressed in *Escherichia coli*, specifically digests IgG1 below the hinge region and generates  $\text{F}(\text{ab}')_2$  and scFc fragments (Figure 1a). In our experiment, IgG1 and IdeS were preloaded in two syringes separately (Figure 1b). Both syringes were pumped at a flow rate of 5  $\mu\text{L}/\text{min}$ , and the reactants were brought together in a mixing Tee connected to a sprayer via a piece of 2 cm fused-silica capillary.

The mixed sample was sprayed for 5 min, and the microdroplets were collected into a vial containing 1% FA in water as a quenching solvent (IdeS is inactivated at pH < 5). The vial lid was closed, and a hole was drilled on the lid to allow the insertion of the sprayer tip into the vial for spray. The distance between the sprayer and the quenching solution in the vial was 2 cm, and the speed of the sprayed microdroplets was  $84 \pm 18$  m/s as previously measured.<sup>14</sup> Thus, the flight time of the microdroplet between the sprayer and the quenching solution was only 250  $\mu\text{s}$  [ $2 \text{ cm}/(84 \text{ m/s}) \cong 250 \mu\text{s}$ ]. Even in such a short spray time, we achieved optimal digestion efficiency of the antibody in the microdroplets. The collected sample was desalted and analyzed by nESI MS (see the workflow shown in Figure 1b). Figure 1c shows that all IdeS-cleaved subunits [i.e.,  $\text{F}(\text{ab}')_2$  and scFc] were clearly observed in the MS spectra. In addition, we efficiently detected and resolved different glycoforms (G0F, G1F, and G2F) of scFc fragments (sequence coverage 100%). Furthermore, we did not observe any remaining intact IgG1 after microdroplet digestion, which indicated 100% digestion efficiency in microdroplets. In addition, 100% digestion efficiency was obtained during nine individual runs, suggesting the high reproducibility of IdeS digestion of IgG1 in microdroplets (see the deconvoluted MS spectra in Figure S1, Supporting Information). The time of 250  $\mu\text{s}$  in microdroplets for completely digesting an intact antibody at 25  $^\circ\text{C}$  represented a 7.5 million-fold speed improvement in comparison with traditional digestion in bulk solution that requires at least 30 min to 1 h at 37  $^\circ\text{C}$ .<sup>45</sup> To prove that IgG1 was truly digested in microdroplets during the spray process (Figure 1b), we also

conducted a control experiment in which 1 mg/mL IgG1 was mixed and incubated with 2 units/ $\mu$ L IdeS (the same concentrations as used in the microdroplet digestion) in solution for digestion at 37 °C for 5 min, and no notable digestion was observed (Figure 1d). Clearly, the microdroplets did markedly accelerate enzymatic digestion of the intact antibody. Note that, in Figure 1b of the microdroplet experiment, the residual time of IgG1 and IdeS in the 2 cm connection capillary after Tee mixing was only 4.4 s (see calculation in the Supporting Information), which we did not expect to lead to noticeable digestion inside the capillary. Furthermore, we halved the amount of IdeS in the microdroplet digestion of IgG1 (1 unit IdeS for 1  $\mu$ g of IgG1), and 100% digestion efficiency was still obtained in nine individual runs (Figure S2, Supporting Information).

Strikingly, we found that adding another reagent into the spray solvent enabled another ultrafast reaction step. For example, addition of the reducing reagent TCEP in the spray solution containing IdeS and IgG1 accelerated disulfide bond reduction of the antibody, leading to simultaneous digestion and reduction of the antibody in the microdroplets, which is illustrated in Figure 2a. Following the workflow shown in Figure 2b, IgG1 and TCEP were premixed in one syringe, and IdeS was preloaded in the other syringe. Both syringes were pumped at a flow rate of 5  $\mu$ L/min. Reactants were mixed via a Tee and transferred to the sprayer for generating microdroplets, which were again directed to a collection vial containing an acidic quenching solution (Figure 2b). After digestion in the microdroplets, we clearly observed all of the digested and reduced fragments, LC, Fd', and glycosylated scFc's including scFc + G0F, scFc + G1F, and scFc + G2F in the MS spectrum (Figure 2c) and the deconvoluted MS spectrum (Figure 2d), with the mass of each fragment within the measurement accuracy (Table S1, Supporting Information). In addition, in the full deconvoluted MS spectrum (Figure S3, Supporting Information), neither the intact antibody nor F(ab')<sub>2</sub> peaks were seen, suggesting that both digestion and reduction were complete. In antibody characterization, reduced fragments are valuable because they are amenable to MS/MS techniques that provide high-sequence coverage and localization of structural modifications.

Besides conducting the microdroplet reaction in an "one-pot reaction" manner as described above, the dual reaction of digestion and reduction could be performed stepwise. According to the stepwise workflow shown in Scheme S1a (Supporting Information), we mixed IgG1 and IdeS via a Tee mixer and sprayed the mixture as microdroplets to digest IgG1. The collected microdroplets were then mixed with TCEP in a vial and sprayed again to accelerate reduction in microdroplets. The F(ab')<sub>2</sub> fragment was further reduced to LC and Fd' fragment. The collected microdroplets were reconstituted and desalted for nESI-MS analysis. Figure S4 (Supporting Information) shows that all IdeS-cleaved and TCEP-reduced subunits (i.e., LC, Fd', and scFc's) were clearly observed in the MS spectra. Different glycoforms (G0F, G1F, and G2F) of scFc fragments were also detected and resolved efficiently. In addition, this workflow successfully digested and reduced IgG1 in phosphate buffer (see Figure S5, Supporting Information), which indicated that microdroplet digestion could be performed in a nonvolatile buffer solution. Likewise, for the stepwise workflow, we could mix IgG1 and TCEP first for microdroplet reduction and then further mix with IdeS for digestion (Scheme S1b, Supporting Information). All IdeS-

cleaved and TCEP-reduced fragments (LC, Fd', and scFc's) were also observed (Figure S6, Supporting Information), suggesting that the reduction and digestion reaction order can be switched.

To accelerate further the analysis process, one can use online MS detection in combination with simultaneous microdroplet digestion and reduction. It would be worthwhile to conduct microdroplet digestion and MS detection simultaneously as a real-time analysis because simultaneous operation would condense the digestion and reduction time to a minimum.<sup>14</sup> For the online workflow, EESI-MS<sup>58–61</sup> was used, in which two sprayers were aligned and used together in the front of the MS inlet (Figure 2e). One sprayer served as the sample sprayer to generate microdroplets containing a mix of IgG1, IdeS, and TCEP without applying any voltage. The other sprayer worked as a solvent sprayer to generate microdroplets of ACN/H<sub>2</sub>O/FA (50:50:0.5%) with +3 kV voltage applied to produce charged solvent microdroplets to assist the ionization of resulting fragments contained in the sample spray microdroplets. The IgG1 was cleaved with IdeS and reduced with TCEP into smaller fragments at the same time in the sample microdroplets in air at room temperature. Charged microdroplets of the solvent mixed with and contacted the sample microdroplets and enabled sample ionization; the LC, Fd', scFc + G0F, scFc + G1F, and scFc + G2F fragments were all detected by online MS analysis (Figure 2f). This approach allowed us to online detect digested and reduced IgG1 fragments directly from the sprayed microdroplets without any sample pretreatment or preparation. We noted a peak at 24,402 Da (asterisked in Figure 2f) corresponding to a harmonic peak of Fab (see the deconvoluted MS spectrum in Figure S7a, Supporting Information) and a small F(ab')<sub>2</sub> peak (Figure S7b, Supporting Information) as well as a small intact antibody peak (Figure S7c, Supporting Information). It is likely that the IdeS digestion of antibody and TCEP reduction for F(ab')<sub>2</sub> were not complete because of the shortened travel distance of the sample microdroplets in the EESI experiment (intercepted by the EESI solvent spray before traveling 20 mm to reach MS inlet) in comparison to the offline experiment described in Figure 2b. Note that the ion intensity of antibody fragments in the online EESI experiment was lower (Figure 2f) in comparison to the offline experiment (Figure 2d). One possible reason is that more water and less organic solvents were sprayed into the MS inlet when using an online EESI-MS approach. Another possible reason is that the excess amount of TCEP and ammonium bicarbonate could reduce the ion signal of antibody fragments as there was no sample purification step in this online process. One possible solution for this issue might be to perform online desalting<sup>62</sup> by increasing the organic solvent composition in the solvent spray of EESI, so that salts from the sample droplets could be excluded in the newly fused secondary droplets for ion generation.

Glycation is a nonenzymatic protein modification that occurs between reducing sugars (e.g., glucose, fructose, and galactose) and proteins.<sup>63</sup> The primary amine groups of lysine residues and the N-termini of proteins react with aldehyde groups from reducing sugars to form Schiff base intermediates, which are further converted via Amadori rearrangement into more stable ketoamines. Glycation has been commonly observed in therapeutic antibodies during manufacturing and storage, and glycation could affect drug product stability, safety, and efficacy.<sup>64</sup> Thus, it is of major importance to characterize and determine the effect of glycation on the mAb

structure. However, conventional methods, such as boronate affinity chromatography, capillary isoelectric focusing, and liquid chromatography–MS, suffer from low throughput because of the required long separation times. Fit-for-purpose assays are still lagging to meet the high-throughput demands of the pharmaceutical industry. It has been stated that the top priority of the US Food and Drug Administration is the development of new tools for high-throughput therapeutic protein characterization.<sup>65</sup>

Consequently, we were motivated to attempt a rapid characterization method for glycosylated IgG1 using microdroplet digestion and reduction. After incubation with glucose, the glycosylated NIST IgG1 underwent microdroplet digestion and reduction in the “one-pot reaction” workflow (i.e., mixing with both IdeS and TCEP), and Figure 3a–c presents the MS spectra of IgG1 obtained after 0, 2, and 5 days of incubation with glucose after microdroplet digestion and reduction. Figure 3a shows the digested and reduced IgG1 fragments from the IgG1 sample without incubation with glucose. After 2 days of incubation, monoglycosylated LC and monoglycosylated Fd' fragments were seen (Figure 3b). With 5 days continued incubation, diglycosylated LC and diglycosylated Fd' fragments were also detected and resolved in the MS spectra (Figure 3c). In addition, after 5 days of incubation, both monoglycosylated LC and Fd' fragments appeared to be more abundant (Figure 3c) in comparison to the sample after 2 days of incubation (Figure 3b). With a longer incubation time, more glycosylated fragments were produced and detected (data not shown). All antibody fragments including mono- and diglycosylated LC and Fd' fragments were detected and resolved in the deconvoluted MS spectrum (Figure 3d) and 2D spectrum (Figure 3e). The microdroplet-based digestion facilitates rapid glycation analysis of mAb subunits subjected to glycation stress. Microdroplet digestion of glycosylated IgG constitutes a proof-of-concept of a method to analyze other modifications of mAbs, such as oxidation, small molecule or peptide conjugation, and sequence variations, truncations, and extensions. Thus, the mAb subunits generated via microdroplets add to the toolbox of methods available for antibody characterization and product quality assessment during development and manufacturing.

Antibody glycosylation is heterogeneous, and variables in cell culture can increase glycan diversity. A conserved *N*-glycan at Asn297 of the scFc region of IgG1 is critical for stability, conformation, aggregation, and effector function of therapeutic antibodies.<sup>66</sup> Removing glycosylation during mass spectrometric analysis would be beneficial to ease the characterization of antibodies and to obtain the correct *N*-linked oligosaccharide (*N*-glycan) profile. *N*-Glycosidase F (PNGase F), a recombinant glycosidase from *Elizabethkingia miricola*, is one of the most effective enzymes to cleave *N*-glycans from proteins (illustrated in Figure 4a). In our experiment, first we preloaded IgG1 and PNGase F in two syringes, respectively (see the workflow in Figure S8, Supporting Information). Both syringes were pumped at a flow rate of 5  $\mu$ L/min, and the reactants were mixed by a Tee and then sprayed to generate microdroplets. The microdroplets were quenched with H<sub>2</sub>O containing 1% FA in the collection vial and collected for 5 min. The distance between the sprayer and the quenching solution was kept as 2 cm. The collected sample was desalted and analyzed by nESI-MS. Figure S8c (Supporting Information) shows the MS spectrum of deglycosylation of IgG1 by PNGase F in microdroplets at ambient temperature. In comparison to the intact IgG1 MS spectrum (Figure S8d, Supporting

Information), new antibody peaks appeared (Figure S8c, Supporting Information). The deconvoluted MS spectrum (Figure S8b, Supporting Information) clearly presents deglycosylated IgG1 peaks and a small amount of IgG1 with one glycan attached. This analysis indicated a high microdroplet reaction efficiency of deglycosylation. The deglycosylation yield for producing fully deglycosylated IgG1 was estimated to be  $96.1 \pm 3.2\%$  (calculated using the ratio of fully deglycosylated IgG1 peak intensity and the sum of the fully deglycosylated IgG1 and the partially deglycosylated IgG1 peak intensities in Figure S8b) based on five individual runs.

We further tested a stepwise workflow in which the IgG1 was first deglycosylated by PNGase F and then reduced and digested by addition of IdeS and TCEP in the second step (Figure S9a). In this workflow, IgG1 and PNGase F were mixed via a Tee and sprayed as microdroplets to remove *N*-glycans from IgG1. Then, the collected microdroplets were mixed with IdeS and TCEP and sprayed again to accelerate reduction and digestion in the microdroplets. The deglycosylated IgG1 was reduced and digested into LC, Fd', and deglycosylated scFc fragments. The collected microdroplets were reconstituted and desalted for nESI-MS analysis. Figure S9b shows that all fragments were observed clearly in the MS spectra. In addition, we did not observe any glycosylated (G0F, G1F, and G2F) scFc fragments; thus, deglycosylation in the microdroplets appeared to be 100% efficient, a fact that was confirmed in the deconvoluted MS spectrum (Figure S9c). Therefore, by conducting deglycosylation in the microdroplets, nonglycosylated antibody fragments can be obtained for rapid structure characterization, thereby avoiding the influence of the complex profiles of the *N*-glycans.

We went on to perform an “one-pot reaction” test, in which IgG1, PNGase F, IdeS, and TCEP were mixed and sprayed for triggering deglycosylation, digestion, and reduction simultaneously in the microdroplets. We observed the LC, Fd', and scFc (both deglycosylated and glycosylated) fragments by nESI-MS analysis after microdroplet reaction and sample collection (Figure 4b,c). Although deglycosylation of scFc was not complete in this trial ( $38.0 \pm 2.6\%$  deglycosylation efficiency in eight individual runs), the results indicated that antibody digestion, deglycosylation, and reduction can occur simultaneously in the microdroplets in a short amount of time (250  $\mu$ s).

## CONCLUSIONS

Currently, microdroplet reactions have been applied to many small-molecule substrates for various purposes, including (1) synthesis of organic products and nanoparticles,<sup>17,67</sup> (2) kinetic measurements,<sup>14</sup> (3) rapid derivatization<sup>1,68</sup> or degradation,<sup>69</sup> and (4) chemical behavior and fundamental studies.<sup>18</sup> Typically, only a one-step reaction was involved in these reported microdroplet reactions. Biochemical reactions in microdroplets were rarely reported so far, with the exception of the syntheses of sugar phosphates and uridine ribonucleoside via condensation<sup>19</sup> and trypsin digestion of peptides and small proteins in microdroplets.<sup>34</sup> Our work represents the first report of multiple-step reactions involving a large protein of intact antibody in microdroplets.

In summary, we demonstrated ultrafast IdeS digestion of intact antibody in microdroplets. We achieved and detected digestion in 250 microseconds, a vastly improved speed compared with conventional in-solution digestion. Further, ultrafast reduction is feasible by doping the spray solvent with

TCEP, leading to the IdeS-cleaved and TCEP-reduced fragments (LC, Fd', and scFc with different glycoforms). Moreover, we have shown that microdroplet digestion can be achieved in both volatile and nonvolatile aqueous buffers; thus, other biochemical reactions are likely to occur in microdroplets. In addition, glycosylated IgG1 after incubation with glucose was digested successfully in microdroplets and analyzed by MS. Furthermore, microdroplet reaction coupled with online EESI-MS analysis would be an alternative approach having the least time for digestion, reduction, and detection without sample pretreatment. We also achieved rapid deglycosylation of IgG1 by the PNGase F enzyme in the microdroplets. Although only NIST IgG1 was selected as a test sample, we believe that all these workflows and approaches are general and will greatly aid in the efforts to reduce the analysis time and improve the throughput of mAb characterization.

## ■ ASSOCIATED CONTENT

### SI Supporting Information

The Supporting Information is available free of charge at <https://pubs.acs.org/doi/10.1021/acs.analchem.0c04974>.

Additional MS spectra, experimental setup, and experimental description (PDF)

## ■ AUTHOR INFORMATION

### Corresponding Authors

**Harsha P. Gunawardena** – Janssen Research & Development, The Janssen Pharmaceutical Companies of Johnson & Johnson, Spring House, Pennsylvania 19477, United States; [orcid.org/0000-0003-3245-3293](https://orcid.org/0000-0003-3245-3293); Email: [hgunawar@ITS.JNJ.com](mailto:hgunawar@ITS.JNJ.com)

**Richard N. Zare** – Department of Chemistry, Stanford University, Stanford, California 94305-5080, United States; [orcid.org/0000-0001-5266-4253](https://orcid.org/0000-0001-5266-4253); Email: [zare@stanford.edu](mailto:zare@stanford.edu)

**Hao Chen** – Department of Chemistry & Environmental Science, New Jersey Institute of Technology, Newark, New Jersey 07102, United States; [orcid.org/0000-0001-8090-8593](https://orcid.org/0000-0001-8090-8593); Email: [hao.chen.2@njit.edu](mailto:hao.chen.2@njit.edu)

### Authors

**Pengyi Zhao** – Department of Chemistry & Environmental Science, New Jersey Institute of Technology, Newark, New Jersey 07102, United States; [orcid.org/0000-0002-7873-1773](https://orcid.org/0000-0002-7873-1773)

**Xiaoqin Zhong** – Department of Chemistry, Fudan University, Shanghai 200438, China

Complete contact information is available at:

<https://pubs.acs.org/doi/10.1021/acs.analchem.0c04974>

### Notes

The authors declare no competing financial interest.

## ■ ACKNOWLEDGMENTS

We thank the National Science Foundation (CHE-1915878) and the National Institute of Health (1R15GM137311-01) for funding. The authors also acknowledge support from Janssen Research & Development.

## ■ REFERENCES

(1) Girod, M.; Moyano, E.; Campbell, D. I.; Cooks, R. G. *Chem. Sci.* **2011**, *2*, 501–510.

(2) Lee, J. K.; Walker, K. L.; Han, H. S.; Kang, J.; Prinz, F. B.; Waymouth, R. M.; Nam, H. G.; Zare, R. N. *Proc. Natl. Acad. Sci. U.S.A.* **2019**, *116*, 19294–19298.

(3) Lee, J. K.; Samanta, D.; Nam, H. G.; Zare, R. N. *J. Am. Chem. Soc.* **2019**, *141*, 10585–10589.

(4) Wei, Z.; Li, Y.; Cooks, R. G.; Yan, X. *Annu. Rev. Phys. Chem.* **2020**, *71*, 31–51.

(5) Yan, X.; Bain, R. M.; Cooks, R. G. *Angew. Chem., Int. Ed.* **2016**, *55*, 12960–12972.

(6) Nie, H.; Wei, Z.; Qiu, L.; Chen, X.; Holden, D. T.; Cooks, R. G. *Chem. Sci.* **2020**, *11*, 2356–2361.

(7) Basuri, P.; Gonzalez, L. E.; Morato, N. M.; Pradeep, T.; Cooks, R. G. *Chem. Sci.* **2020**, *11*, 12686–12694.

(8) Li, Y.; Mehari, T. F.; Wei, Z.; Liu, Y.; Cooks, R. G. *J. Mass Spectrom.* **2020**, No. e4585.

(9) Li, Y.; Yan, X.; Cooks, R. G. *Angew. Chem., Int. Ed.* **2016**, *55*, 3433–3437.

(10) Sahraeian, T.; Kulyk, D. S.; Badu-Tawiah, A. K. *Langmuir* **2019**, *35*, 14451–14457.

(11) Tang, S.; Cheng, H.; Yan, X. *Angew. Chem., Int. Ed.* **2020**, *59*, 209–214.

(12) Vaitheeswaran, S.; Thirumalai, D. J. *Am. Chem. Soc.* **2006**, *128*, 13490–13496.

(13) Sahota, N.; Abusalim, D. I.; Wang, M. L.; Brown, C. J.; Zhang, Z.; El-Baba, T. J.; Cook, S. P.; Clemmer, D. E. *Chem. Sci.* **2019**, *10*, 4822–4827.

(14) Lee, J. K.; Kim, S.; Nam, H. G.; Zare, R. N. *Proc. Natl. Acad. Sci. U.S.A.* **2015**, *112*, 3898–3903.

(15) Cheng, H.; Tang, S.; Yang, T.; Xu, S.; Yan, X. *Angew. Chem., Int. Ed.* **2020**, *59*, 19862–19867.

(16) Bain, R. M.; Sathyamoorthi, S.; Zare, R. N. *Angew. Chem., Int. Ed.* **2017**, *129*, 15279–15283.

(17) Lee, J. K.; Samanta, D.; Nam, H. G.; Zare, R. N. *Nat. Commun.* **2018**, *9*, 1562.

(18) Gnanamani, E.; Yan, X.; Zare, R. N. *Angew. Chem., Int. Ed.* **2020**, *59*, 3069–3072.

(19) Nam, I.; Lee, J. K.; Nam, H. G.; Zare, R. N. *Proc. Natl. Acad. Sci. U.S.A.* **2017**, *114*, 12396–12400.

(20) Banerjee, S.; Zare, R. N. *Angew. Chem., Int. Ed.* **2015**, *54*, 14795–14799.

(21) Gao, D.; Jin, F.; Lee, J. K.; Zare, R. N. *Chem. Sci.* **2019**, *10*, 10974–10978.

(22) Luo, K.; Li, J.; Cao, Y.; Liu, C.; Ge, J.; Chen, H.; Zare, R. N. *Chem. Sci.* **2020**, *11*, 2558–2565.

(23) Banerjee, S.; Gnanamani, E.; Yan, X.; Zare, R. N. *Analyst* **2017**, *142*, 1399–1402.

(24) Marsh, B. M.; Iyer, K.; Cooks, R. G. *J. Am. Soc. Mass Spectrom.* **2019**, *30*, 2022–2030.

(25) Mondal, S.; Acharya, S.; Biswas, R.; Bagchi, B.; Zare, R. N. *J. Chem. Phys.* **2018**, *148*, 244704.

(26) Xiong, H.; Lee, J. K.; Zare, R. N.; Min, W. J. *Phys. Chem. Lett.* **2020**, *11*, 7423–7428.

(27) Chamberlayne, C. F.; Zare, R. N. *J. Chem. Phys.* **2020**, *152*, 184702.

(28) Tuck, A. F. *Entropy* **2019**, *21*, 1044.

(29) Xiong, H.; Lee, J. K.; Zare, R. N.; Min, W. J. *Phys. Chem. B* **2020**, *124*, 9938–9944.

(30) Chamberlayne, C. F.; Zare, R. N.; Santiago, J. G. *J. Phys. Chem. Lett.* **2020**, *11*, 8302–8306.

(31) Narendra, N.; Chen, X.; Wang, J.; Charles, J.; Cooks, R. G.; Kubis, T. *J. Phys. Chem. A* **2020**, *124*, 4984–4989.

(32) Zhou, Z.; Yan, X.; Lai, Y.-H.; Zare, R. N. *J. Phys. Chem. Lett.* **2018**, *9*, 2928–2932.

(33) Rovelli, G.; Jacobs, M. I.; Willis, M. D.; Rapf, R. J.; Prophet, A. M.; Wilson, K. R. *Chem. Sci.* **2020**, *11*, 13026–13043.

(34) Zhong, X.; Chen, H.; Zare, R. N. *Nat. Commun.* **2020**, *11*, 1049.

(35) Tsumoto, K.; Isozaki, Y.; Yagami, H.; Tomita, M. *Immunotherapy* **2019**, *11*, 119–127.

- (36) Kaplon, H.; Muralidharan, M.; Schneider, Z.; Reichert, J. M. *mAbs* **2020**, *12*, 1703531.
- (37) Carter, P. J.; Lazar, G. A. *Nat. Rev. Drug Discovery* **2018**, *17*, 197–223.
- (38) Fisher, A. C.; Lee, S. L.; Harris, D. P.; Buhse, L.; Kozlowski, S.; Yu, L.; Kopcha, M.; Woodcock, J. *Int. J. Pharm.* **2016**, *515*, 390–402.
- (39) Nagy, G.; Attah, I. K.; Conant, C. R.; Liu, W.; Garimella, S. V. B.; Gunawardena, H. P.; Shaw, J. B.; Smith, R. D.; Ibrahim, Y. M. *Anal. Chem.* **2020**, *92*, 5004–5012.
- (40) Beck, A.; Wagner-Rousset, E.; Ayoub, D.; Van Dorsselaer, A.; Sanglier-Cianféran, S. *Anal. Chem.* **2013**, *85*, 715–736.
- (41) Kang, L.; Weng, N.; Jian, W. *Biomed. Chromatogr.* **2020**, *34*, No. e4633.
- (42) Jin, Y.; Lin, Z.; Xu, Q.; Fu, C.; Zhang, Z.; Zhang, Q.; Pritts, W. A.; Ge, Y. *mAbs* **2019**, *11*, 106–115.
- (43) Donnelly, D. P.; Rawlins, C. M.; DeHart, C. J.; Fornelli, L.; Schachner, L. F.; Lin, Z.; Lippens, J. L.; Aluri, K. C.; Sarin, R.; Chen, B.; Lantz, C.; Jung, W.; Johnson, K. R.; Koller, A.; Wolff, J. J.; Campuzano, I. D. G.; Auclair, J. R.; Ivanov, A. R.; Whitelegge, J. P.; Paša-Tolić, L.; Chamot-Rooke, J.; Danis, P. O.; Smith, L. M.; Tsybin, Y. O.; Loo, J. A.; Ge, Y.; Kelleher, N. L.; Agar, J. N. *Nat. Methods* **2019**, *16*, 587–594.
- (44) Lodge, J. M.; Schauer, K. L.; Brademan, D. R.; Riley, N. M.; Shishkova, E.; Westphall, M. S.; Coon, J. J. *Anal. Chem.* **2020**, *92*, 10246–10251.
- (45) An, Y.; Zhang, Y.; Mueller, H.-M.; Shameem, M.; Chen, X. *mAbs* **2014**, *6*, 879–893.
- (46) Huang, L.; Wang, N.; Mitchell, C. E.; Brownlee, T.; Maple, S. R.; De Felippis, M. R. *Anal. Chem.* **2017**, *89*, 5436–5444.
- (47) Fekete, S.; Guillarme, D.; Sandra, P.; Sandra, K. *Anal. Chem.* **2016**, *88*, 480–507.
- (48) Mouchahoir, T.; Schiel, J. E. *Anal. Bioanal. Chem.* **2018**, *410*, 2111–2126.
- (49) Carvalho, L. B.; Capelo-Martínez, J.-L.; Lodeiro, C.; Wiśniewski, J. R.; Santos, H. M. *Anal. Chem.* **2020**, *92*, 9164–9171.
- (50) Rivera-Albarran, M. E.; Ray, S. J. *J. Am. Soc. Mass Spectrom.* **2020**, *31*, 1684–1696.
- (51) Basile, F.; Hauser, N. *Anal. Chem.* **2011**, *83*, 359–367.
- (52) López-Ferrer, D.; Capelo, J. L.; Vázquez, J. J. *Proteome Res.* **2005**, *4*, 1569–1574.
- (53) Russell, W. K.; Park, Z.-Y.; Russell, D. H. *Anal. Chem.* **2001**, *73*, 2682–2685.
- (54) Ji, J.; Zhang, Y.; Zhou, X.; Kong, J.; Tang, Y.; Liu, B. *Anal. Chem.* **2008**, *80*, 2457–2463.
- (55) Bark, S. J.; Muster, N.; Yates, J. R.; Siuzdak, G. *J. Am. Chem. Soc.* **2001**, *123*, 1774–1775.
- (56) Wang, Y.; Zhang, W.; Ouyang, Z. *Chem. Sci.* **2020**, *11*, 10506–10516.
- (57) Takáts, Z.; Wiseman, J. M.; Gologan, B.; Cooks, R. G. *Anal. Chem.* **2004**, *76*, 4050–4058.
- (58) Chen, H.; Yang, S.; Li, M.; Hu, B.; Li, J.; Wang, J. *Angew. Chem., Int. Ed.* **2010**, *49*, 3053–3056.
- (59) Chen, H.; Venter, A.; Cooks, R. G. *Chem. Commun.* **2006**, 2042–2044.
- (60) Chen, H.; Gamez, G.; Zenobi, R. *J. Am. Soc. Mass Spectrom.* **2009**, *20*, 1947–1963.
- (61) Chen, H.; Yang, S.; Wortmann, A.; Zenobi, R. *Angew. Chem., Int. Ed.* **2007**, *46*, 7591–7594.
- (62) Miao, Z.; Chen, H. *J. Am. Soc. Mass Spectrom.* **2009**, *20*, 10–19.
- (63) Quan, C.; Alcalá, E.; Petkovska, I.; Matthews, D.; Canova-Davis, E.; Taticek, R.; Ma, S. *Anal. Biochem.* **2008**, *373*, 179–191.
- (64) Wei, B.; Berning, K.; Quan, C.; Zhang, Y. T. *mAbs* **2017**, *9*, 586–594.
- (65) Woodcock, J.; Woosley, R. *Annu. Rev. Med.* **2008**, *59*, 1–12.
- (66) Jefferis, R. *Nat. Rev. Drug Discovery* **2009**, *8*, 226–234.
- (67) Espy, R. D.; Wleklinski, M.; Yan, X.; Cooks, R. G. *TrAC, Trends Anal. Chem.* **2014**, *57*, 135–146.
- (68) Chen, H.; Cotte-Rodríguez, I.; Cooks, R. G. *Chem. Commun.* **2006**, 597–599.
- (69) Li, Y.; Hu, Y.; Logsdon, D. L.; Liu, Y.; Zhao, Y.; Cooks, R. G. *Pharm. Res.* **2020**, *37*, 138.